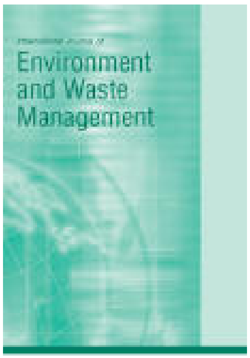

International Journal of Environment and Waste Management

ISSN online: 1478-9868 - ISSN print: 1478-9876
https://www.inderscience.com/ijewm

Application of graphene oxide for fluoride removal: kinetic and isotherm study

Ram Ashok Konale, Nilesh Keshavrao Mahale, Sopan Tukaram Ingle

DOI: 10.1504/IJEWM.2023.10044501

Article History:

Received:	23 November 2020
Accepted:	12 July 2021
Published online:	09 January 2024

Application of graphene oxide for fluoride removal: kinetic and isotherm study

Ram Ashok Konale*,
Nilesh Keshavrao Mahale and
Sopan Tukaram Ingle

School of Environmental and Earth Sciences,
Kavayitri Bahinabai Chaudhari North Maharashtra University,
Umavi Nagar, 425001, Jalgaon, India
Email: ramkonale@gmail.com
Email: nileshmahale@gmail.com
Email: sopan.ingle@gmail.com
*Corresponding author

Abstract: In the present study, graphene oxide (GO) is utilised as an adsorbent for defluoridation from synthetic sample as well as fluorite mine water. A modified Hummers method was adopted for the GO synthesis. The physico-chemical characterisation of the GO was done with FTIR, XRD, FESEM and EDX. The various parameter viz. adsorbent doses (100–250 mg/L), contact time (5–90 min.), pH (2–10), temperature (298–318 K) and initial concentration of fluoride (1–32 mg/L) were optimised for by GO. The maximum 98.34% fluoride adsorption was achieved by 100 mg/L GO dose in 30 min at pH 6. The adsorption process obeys the pseudo second order kinetics ($R^2 = 0.995$), Langmuir (18.86 mg/g) and defluoridation Freundlich isotherm (6.15 L/mg). The ionic interference was found negligible on fluoride removal from the fluorite mine water sample.

Keywords: fluoride adsorption; graphene oxide; kinetic equation; adsorption isotherm model.

Reference to this paper should be made as follows: Konale, R.A., Mahale, N.K. and Ingle, S.T. (2024) 'Application of graphene oxide for fluoride removal: kinetic and isotherm study', *Int. J. Environment and Waste Management*, Vol. 33, No. 1, pp.102–131.

Biographical notes: Ram Ashok Konale obtained his Master's in Environmental Science from the Solapur University, in 2016. He is pursuing his PhD at the KBC North Maharashtra University, Jalgaon. The prime focus of his research is exploration of applications of graphene nanocomposites for water purification and energy exploration. He is working on applications of graphene for water purification and development of energy storage devices. He is also engaged in soil, air pollution remediation with the help of nano materials.

Nilesh Keshavrao Mahale is a former UGC-RFSMS Fellow. He holds a PhD in Environmental Sciences with more than ten years research experience in environmental and energy related areas. At present, he is an IFC Associate at the National Research Development Corporation supported Innovation Facilitation Centre located at KBC North Maharashtra University, Jalgaon, India. His research focuses on development of nanomaterials including scalable

graphene synthesis, nanofibres, nanocomposites and electrocatalysts for various energy and environmental applications like, green hydrogen production, energy storage, water treatment and other aspects of clean and sustainable green energy.

Sopan Tukaram Ingle is a Senior Professor at the School of Environmental and Earth Sciences, KBC North Maharashtra University, Jalgaon. He completed his PhD in Environmental Biology from the Mumbai University, Mumbai, in 1992. He has expertise in air, and noise pollution monitoring, health impacts assessment and occupational health hazards. Presently, he is engaged with the sustainable energy exploration. He has over 50 Scopus and Web of Science indexed publications in reputed, high impact factor journals. In addition, he has involved in the research related to socio-economic and environmental impacts assessment of developmental activities.

1 Introduction

Fluoride is recognised as the thirteenth most common element in the earth's crust. It is widely distributed in the lithosphere mainly as fluorspar, fluorapatite and cryolite. It is also found in seawater at a concentration of around 1.2–1.4 mg/L, and in groundwater up to 67 mg/L (WHO, 2004). The igneous and sedimentary rocks are some of the geological sources of fluoride, the concentration ranges 0.06% to 0.09% in the upper lithosphere of these igneous and sedimentary rocks (Athanasia et al., 2019; Jayarathna et al., 2015; Li et al., 2013). The physical and biological activities in these fluoride containing rocks lead to the leaching of the fluoride ions in the ground and surface water bodies (Chiavola et al., 2019; Nigri et al., 2017; Malana et al., 2014). Apart from leaching, geochemical reactions and volcanic eruptions are also some of the natural causes of fluoride-contamination. Anthropogenic sources of fluoride release in the environment includes fluorite mining, aluminium electrolysis, thermal power plants, semiconductor processing, electroplating, thermal power plants, pharmaceuticals, rubber and fertiliser production (Dhillon et al., 2017; Biswas et al., 2017).

The long-term fluoride exposure from 6 to 14 mg/L per day leads to skeletal fluorosis, bone deformation and increased risk of bone fractures (WHO, 2004). As per the World Health Organization (WHO), the 1.5 mg/L is the permissible limit for fluoride concentration in drinking water (Augustine and Pius, 2017; Manikandan et al., 2013). Fluoride concentration above permissible limit in drinking water leads to skeletal fluorosis (Esmeralda et al., 2019; Hernandez et al., 2019; Corral et al., 2019), thyroid, cardiovascular and neurological problems (Manna et al., 2018), high blood pressure and lower fertility (Ingallinella et al., 2011 Gogoi et al., 2018). Fluoride is also associated with Alzheimer's disease, low IQ, and mental retardation at high concentration (Tomar and Kumar, 2013). In more severe forms, symptoms of these diseases include chronic joint pain, similar to the early symptoms of arthritis and excess fluoride destroys the function of the thyroid gland (Zhang et al., 2018; Wu et al., 2018; Vardhan and Srimurali, 2016).

The high amount of fluoride in the water is reported in 12 states of India. Assam (1.6–29 mg/L), Bihar (0.2–8.32 mg/L), West Bengal (1.1–14.47 mg/L), Haryana (0.23–18 mg/L), Madhya Pradesh (1.5–4.2 mg/L), Uttar Pradesh (0.2–25 mg/L), Panjab

(0.4–42 mg/L), Gujrat (1.5–18 mg/L), Maharashtra (0.11–10 mg/L), Tamil Nadu (0.1–7 mg/L), Andhra Pradesh (0.4–29 mg/L) and Karnataka (0.2–7.7 mg/L) was reported (Gogoi et al., 2018; Singh et al., 2020; Rao et al., 2014). In Maharashtra, some parts of Nagpur, Chandrapur, Yavatmal, Nanded, Akola and Amaravati having groundwater fluoride concentration > 1.5 mg/L and is attributed to the pre-Deccan Trap rocks exposure in these districts (Duraiswami and Patankar, 2011).

The fluoride affected areas are mostly rural, and the groundwater is mainly used for the drinking and agricultural purpose, the high concentrations of fluoride adversely affect human health (Ezzeddine et al., 2014; Dehghani et al., 2018; Kimambo et al., 2019). Manikandan et al. (2013) have reported, worldwide more than 200 million people consumes water containing high amount (> 1.5 mg/L) of fluoride.

Various methods like coagulation, separation, precipitation, absorption, adsorption and reverse osmosis have been used for fluoride removal from water (Yin et al., 2015; Minju et al., 2013; Mesquita et al., 2011; Ahmaruzzaman and Gupta, 2011). Among these defluoridation by adsorption is the most reliable one due to high efficiency, cost-effectiveness and easy operation (Nabbou et al., 2018; Alexander et al., 2018; Bhaumik and Mondal, 2015).

In water treatment, GO is a promising adsorbent material. Graphene oxide, a single atomic plane layer of graphite-oxide is a potentially strong adsorbent (Martinez et al., 2019; Tabish et al., 2018). GO contains many active oxygen functional groups, which makes GO a strong aspirant for fluoride adsorption application (Konale et al., 2020; Kuang et al., 2017; Li et al., 2011).

The present study aims to develop efficient and cost-effective techniques for fluoride decontamination from the drinking water. In the experiments, various parameters viz. initial fluoride concentration, adsorbent doses, contact time, pH and temperature were optimised for fluoride adsorption on GO. The experimental data was verified with different isotherms and kinetic study was also performed in order to understand the adsorption mechanism.

2 Materials and methods

2.1 Chemicals and materials

Sodium nitrate ($NaNO_3$), graphite powder, sodium hydroxide (NaOH), hydrochloric acid (HCl) and potassium permanganate ($KMnO_4$) was procured from fisher scientific, India. Hydrogen peroxide (H_2O_2), and sulphuric acid (H_2SO_4) was supplied by Merck Specialities Pvt. Ltd. All regents are of AR grade and used without further purification.

2.2 Synthesis of graphene oxide

GO was synthesised by some modifications in Hummers method, graphite powder (3 g), and sodium nitrate (1.5 g) as oxidising agent were mixed in 69 ml conc. H_2SO_4 in round bottom flask (RBF) and kept on a magnetic stirrer for 20 min at less than 5°C temperature. After 20 minutes, 9 g $KMnO_4$ was slowly added for 1 hour, the round bottom flask was kept on a water bath at 35°C and stirred for 7 hrs. After the first oxidation step addition of another $KMnO_4$ dispersed slowly for 15 min and the reaction was stirred for 7 hrs, the suspension turned brown, indicating the complete oxidation. The reaction mixture was cooled at room temperature and 300 ml deionised water was added. The suspension was turned to dark brown (Mahale and Ingle 2017; Yu et al., 2016; Marcano et al., 2010). Finally, this brown suspension was further treated with H_2O_2 until the colour turned pale yellow. The residue was washed with 5% HCl followed by deionised water until the neutral pH is attained. Thereafter the GO suspension was continuous sonicated for 3 hours. The sonicated suspension was centrifuged for 15 min at 8,000 rpm to remove excess water, the mother liquor was tested on atomic adsorption spectrophotometer to confirm the Mn free GO is synthesised. The centrifuged GO was dried at 45°C for 2 days, grounded and the powder was stored for later use.

Figure 1 Graphical abstract (see online version for colours)

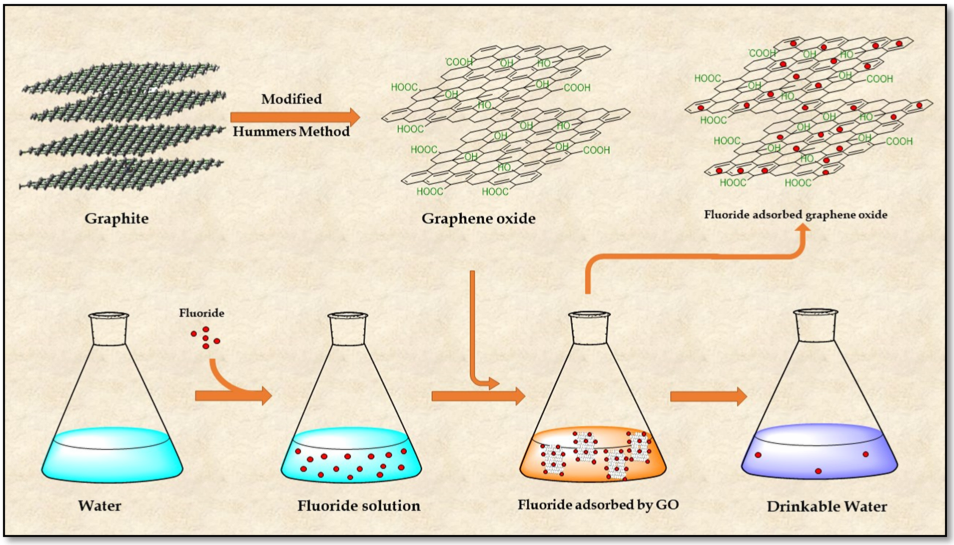

3 Characterisation of the adsorbent

The samples were analysed by Fourier transformation infrared spectroscopy (FTIR) (Shimadzu IR affinity-1) employed with peak intensity range from 400–4,000 cm^{-1}. The XRD pattern were recorded by X-ray diffractometer (LabX XRD-6100) with monochromatised Cu-Ka ($\lambda = 0.154056$ nm) radiation, at 36 kV and 20 mA, sample were scanned in the range 5–80° with continuous scanning mode and scanning speed was set to be 2°/min. The morphological characteristic observed by using field emission scanning electron microscopy (Hitachi FESEM S-4800) under an accelerating voltage of 20 keV, the elemental composition of the sample was carried out using EDX (Bruker Nano). The fluoride concentration was determined by reacting fluoride with a red zirconium-dye solution, i.e., sodium-2-parasulphophenylazo-1-8-dihydroxy-3, 8 naphthalene disulphonate (SPADNS) method. In this method, fluoride combines with part of the zirconium to form a colourless complex, thus bleaching the red colour in an amount proportional to the fluoride concentration. The optical density of the coloured complex was measured at 570 nm wavelength on UV-Vis spectrophotometer.

3.1 Batch adsorption study

Standard fluoride solution was prepared by dissolving 0.221 gm Sodium fluoride in 1,000 ml distilled water. The working standard solutions of fluoride were prepared by serial dilution of standard stock solution. In the adsorption experiment, an appropriate amount of the GO (100–250 mg/L) was added into a solution containing different concentration of fluoride (1–32 mg/L) under continuous stirring. After particular time interval (5–90 min), the adsorbent was separated from the solution by filtration and concentration of the residual fluoride was estimated by SPADNS methods on a UV-visible spectrophotometer at 570 nm (Vardhan and Srimurali 2016; Alipanahpour et al., 2015; Saleh and Gupta 2011; APHA et al., 1996). The residual fluoride estimation was performed three times and mean values were taken for the calculation. The adsorption of fluoride by the GO was calculated using equation (1).

$$\textit{Fluoride removal } \% = \frac{(C_0 - C_t)}{C_0} * 100 \qquad (1)$$

where C_0 is the initial fluoride concentration in water (mg/L), C_t is the equilibrium concentration of fluoride at time t (Asfaram et al., 2016; Saravanan et al., 2013a; Marcano et al., 2010). The adsorption equilibrium capacity of GO was calculated by equation (2).

$$q_t = \frac{(C_0 - C_t)m}{V} \qquad 2$$

where q_t is the equilibrium adsorption capacity, V represent the volume of fluoride solution and m is the mass of GO.

Figure 2 Fourier transform infrared of graphite and graphene oxide (see online version for colours)

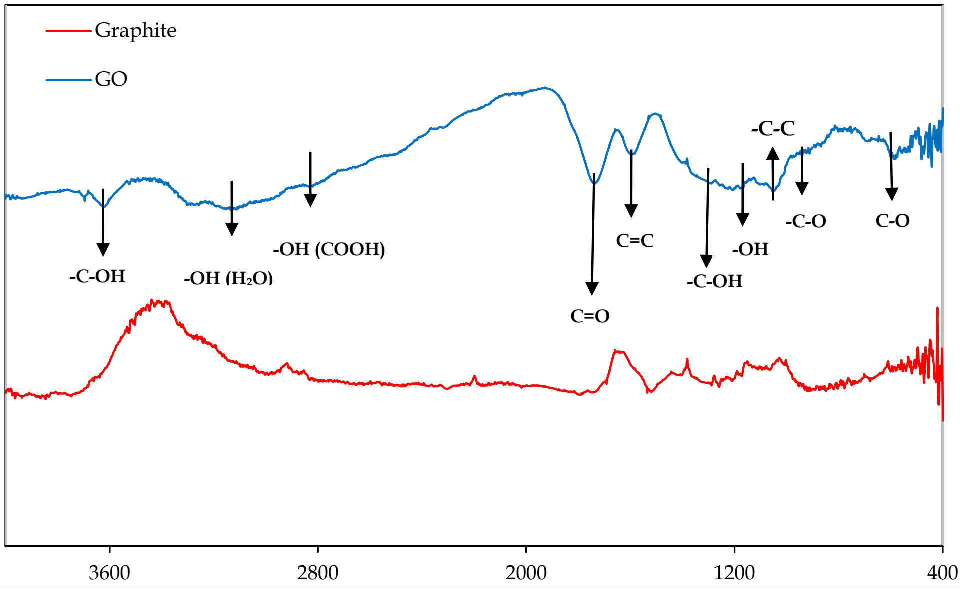

4 Result and discussion

The FTIR analysis was done for identification of functional groups present on graphene oxide. The analysis graph shows bands at 3,620 cm^{-1}, 3,490 cm^{-1}, and 3,190 cm^{-1} all these bands correspond to the residual water molecules adsorbed on the GO.

The band at 2,833 cm^{-1} corresponds to -OH from carboxylic group. A strong characteristic band for C = O of carbonyl group is found at 1,737 cm^{-1}. The aromatic C = C group can be observed at 1,574 cm^{-1}. The -C-OH group is traceable at 1,368 cm^{-1}, the phenolic –OH bending is vivid at 1,196 cm^{-1}, the skeletal -C-C- is a sharp band at 1,053 cm^{-1}. The bands for skeletal C-O are present from 968 to 698 cm^{-1}. In short, the GO having covalently attached oxygen-containing functional groups such as carboxyl, hydroxyl, epoxy and carbonyl groups (Mudila et al., 2016). Hence, the FTIR result confirms the oxidation of graphite by the Hummer's method has induced carboxyl, hydroxyl, epoxy and carbonyl functional groups to the graphene sheets.

5 XRD analysis

The structural characteristic changes occurred during the transformation of graphite to graphene oxide, and these changes are studied using X-ray diffraction patterns. Figure 3 shows the XRD diffraction peaks of graphite and GO. The strong peak of graphite at 27°C indicates that the graphite is of crystalline form and consistent (002) plane due to highly ordered stacking of thick sheets (Xie et al., 2015). XRD patterns of GO indicates the amorphous nature, it shows a sharp peak at $2\theta = 10.2°$, corresponds to the interplanar distance between GO sheets. These peaks change when the conversion of graphite to GO occurs by the increase in the interlayer spacing of intercalation of oxygen-containing functional groups.

Figure 3 XRD pattern of graphite and graphene oxides (see online version for colours)

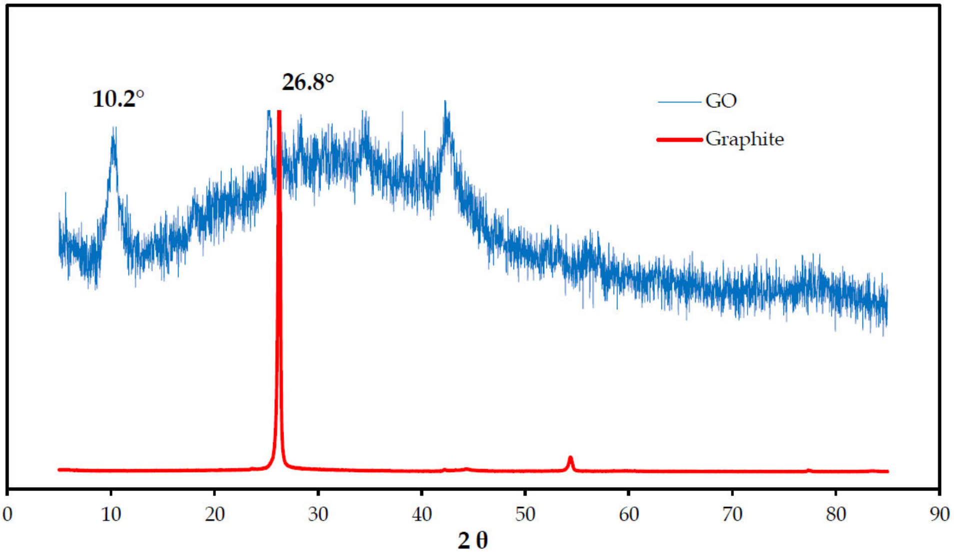

6 Morphology study

The morphology of graphite and GO was studied on FE-SEM. Figures 4(a) and 4(b) show the FESEM results of graphite and GO respectively. Figure 4(b) show a smooth surface with overlapped sheets. It is a two-dimensional sheet-like structure. The GO has multiple wrinkled structures and vivid edges of individual sheets, these sheets are stacked one above other (Xia et al., 2015). The individual GO sheets were found to have a thickness of 1–2 μ and are found to be much larger than the single-layer graphene. From the EDX analysis in Figure 5(b), it is evident that the GO contains around 40.69 % C and 32.01% O which confirms the oxidation of graphite [Figure 5(a)].

Figure 4 (a) FESEM images graphite (b) Graphene oxide

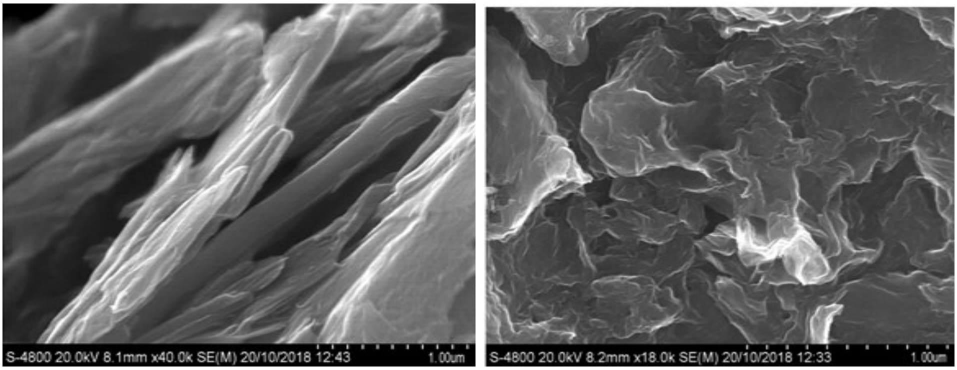

(a) (b)

Figure 5 (a) EDX of graphite (b) Graphene oxide (see online version for colours)

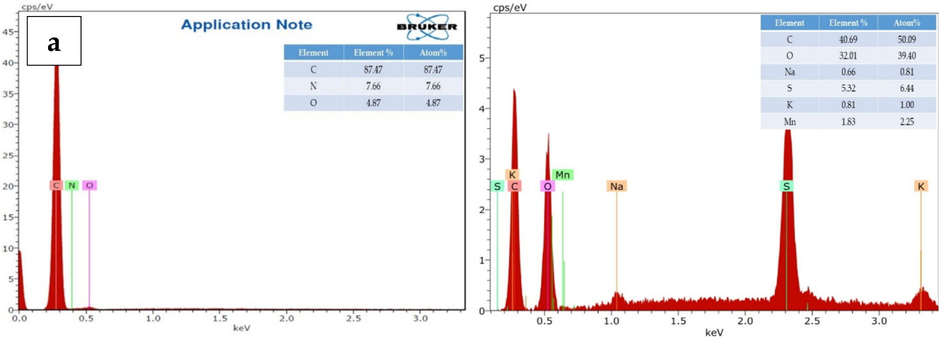

Element	Element %	Atom%
C	87.47	87.47
N	7.66	7.66
O	4.87	4.87

Element	Element %	Atom%
C	40.69	50.09
O	32.01	39.40
Na	0.66	0.81
S	5.32	6.44
K	0.81	1.00
Mn	1.83	2.25

(a) (b)

7 BET surface area and pore distribution analysis

In order to find out the specific surface area of the GO the Brunauer Emmett Teller (BET) analysis was carried out at –198°C. Figure 6(a) reveals the nitrogen adsorption-desorption-isotherms. The porous texture of GO was determined using Barret-Joyner-Halenda (BJH) method results can be seen in Figure 6(b).

Figure 6 (a) Brunaueremmett teller-nitrogen adsorption-desorption isotherm (b) Pore size distribution of the graphene oxide (see online version for colours)

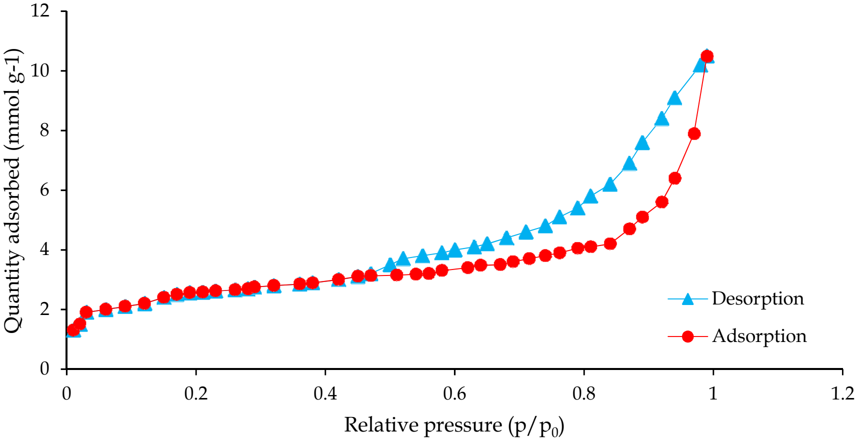

(a)

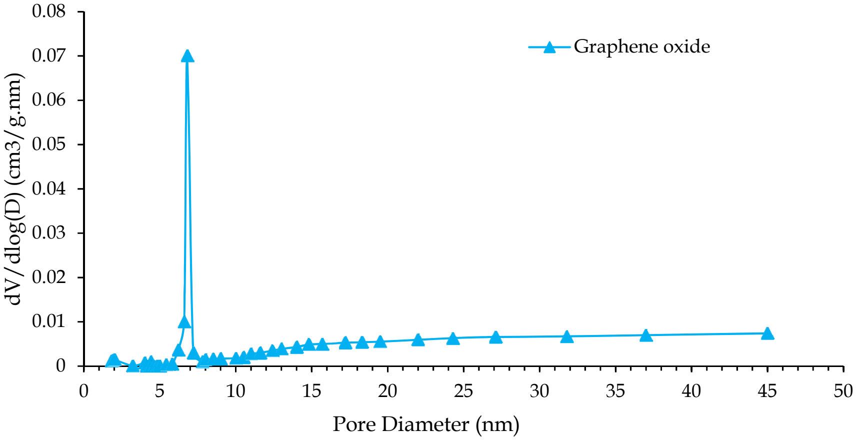

(b)

The nitrogen adsorption-desorption isotherm found of type IV isotherm as per IUPAC classification. The GO demonstrates vertical uptake under P/P = 0.07 and hysteresis loop from P/P = 0.55 to P/P = 1.0. This may be an effect of co-existence of both micro and mesopores. The porous nature of GO with large surface would provide more active sites and improve the fluoride adsorption. The BJH model suggest the maximum number of pores are having < 7 nm size on graphene oxide. The GO possesses BET surface area of 479 m^2/g. The impurity of nitrogen makes graphene easily aligned in layered framework with high surface area (Zhou et al., 2015; Saravanan et al., 2012). Micropore area of the GO was found 327 m^2/g, while 0.341 cm^3/g and micropore volume 0.157 cm^3/g.

8 Effect of pH variation on adsorption of fluoride

Effect of pH on adsorption of fluoride were carried out using adsorbent dose 100 mg/L and fluoride concentration was 2 mg/L at 298 K temperature. The adsorption of fluoride is pH controlled and directly affected by the functional groups present on the surface. The surface charge on the graphene sheet is mostly govern by the pH of the solution. The adsorption efficiency of an adsorbent depends on the textural and chemical characteristic (Ghosh et al., 2016; Gupta et al., 2013). In the adsorption process, the chemical composition of the adsorbent (GO) change in various pH. The pH value of the working solution may influence fluoride adsorption by GO. By increasing the pH from 5 to 6, the fluoride adsorption increases on graphene oxide. At lower pH (2–4) and higher (pH 7–10) the fluoride removal decreases, while the maximum adsorption was occurred at pH 6 (Figure 7) it may be the effect of electrostatic attraction between positively charged GO sheets and negatively charged fluoride ion (Gupta et al., 2015).

Figure 7 Variation of adsorption efficiency with pH (see online version for colours)

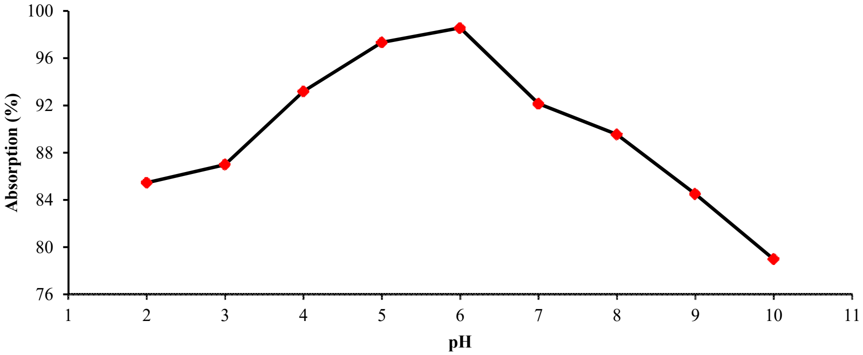

Note: Fluoride concentration 2 mg/l and GO dose 100 mg/l.

Favourable adsorption in the acidic state is possibly due to the interaction between OH^- and F^- on the active surface of adsorbent (Khorshidi and Azadmehr 2016). The observed results can be explained by the complex surface formation theory (CSF), which illustrates that the absorption of inorganic species on solid surfaces results from electrical interaction (Bajpai et al., 2017). In acidic pH, the GO sheet takes positive charge, while the negatively charged hydroxyl ions dominate the adsorption over fluoride ion, this results inhibition of the adsorption of fluoride ions on the GO.

9 Point of zero charge (pH_{zpc})

To find out the influence of pH on adsorption and a potential mechanism for the interaction between GO and fluoride ions the point of zero charge was studied. In this, the pH of the working solution was adjusted from 2 to 10 by addition of diluted solution of NaOH and HCl. In this study the adsorbent dose (GO) was 100 mg/L and fluoride concentration was 2 mg/L at 298 K temperature were kept. The interaction with F^- and GO depends on the pH of working solution, the existence of GO in various forms and pH (zpc) or adsorbent surface charge (Barathi et al., 2014; Gupta et al., 2002). The adsorbent gains neutral charge from acidic solution is referred to as zero-point charge (pHzpc) and it is calculated by batch equilibrium method. Zero-point charge of GO was determined by equation (3).

The surface pH of a neutral charge size is referred to as zero charge and can be calculated in a batch balance manner.

$$\Delta pH = \frac{(pH\ Initial - pH\ Final)}{pH\ Initial} \tag{3}$$

The zero-point charge is one of the most important variables which indicates the adsorption ability on the surface of the GO. The ionic pollutants adsorption on GO is pH dependent. At pH less than pH of zpc the GO surface is positively charged, i.e., in acidic conditions the GO sheets are positively charged and this can attract negatively charged pollutants effectively, this condition is non-favourable for the cationic pollutants due to electrostatic repulsion. On the other hand, pH greater than pHzpc, the GO is negatively charged, this condition is favourable for the electrostatic attraction of cationic pollutants (Imran et al., 2012; Gupta et al., 2011). Overall, the fluoride adsorption is strongly favourable at pH 6. At pH < 6 is not favourable for the fluoride adsorption, as the low pH induces stronger positive charge on the GO sheets, and the hydroxyl ions are more affinitive than fluoride. Figure 8 shows the zpc for GO at pH 7.1 which indicates that the surface of GO is positive below zpc and negative above the zpc. The basic condition is non favourable for the fluoride removal by GO at pH higher than zpc (Mukhopadhyay et al., 2019).

Figure 8 Zero-point charge of GO (see online version for colours)

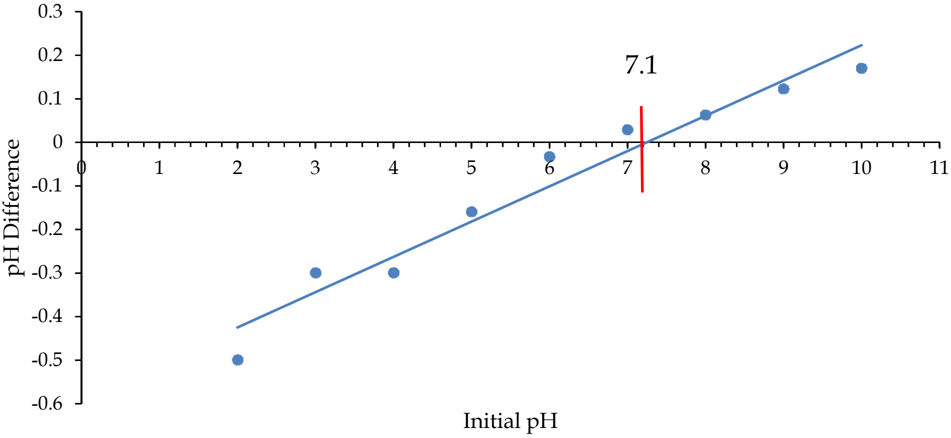

10 Effect of contact time

To study the effect of contact time on adsorption process were estimated using adsorbent dose 100 mg/L and fluoride concentration 2 mg/L at pH 6, 298 K temperature. Figure 9 shows the relationship between contact time and fluoride removal (%). The fluoride removal was rapid between 5–30 min thereafter adsorption rate was slower and finally attains saturation. The rapid adsorption within 30 min could be due to large surface area and high reactivity between fluoride and GO surface over short time (Mudzielwana et al., 2017; Gupta et al., 2014a).

Figure 9 Effect of contact time on removal of fluoride by GO (see online version for colours)

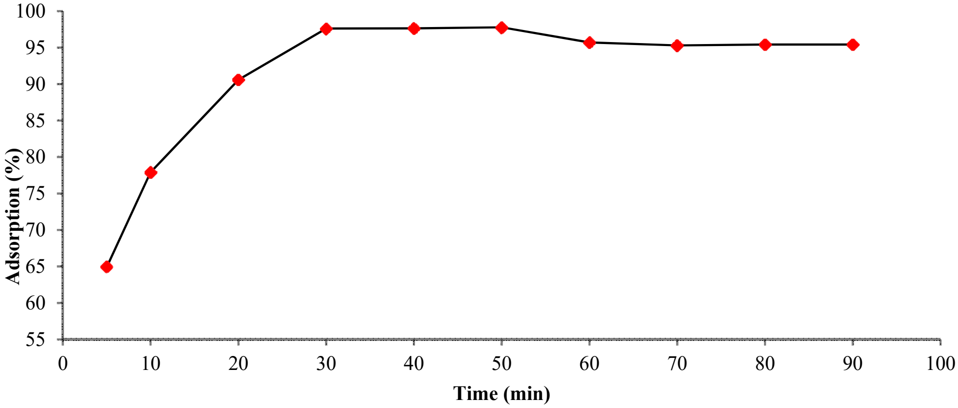

Note: 100 mg/l adsorbent dose and 2 mg/l fluoride concentration.

11 Effect of initial concentration of fluoride

In the present study, the effect of the initial concentration of fluoride and adsorption by GO was investigated using six different concentration of fluoride (1, 2, 4, 8, 16 and 32 mg/L) and adsorbent doses (100–250 mg/L). Figure 9 shows the effect of initial fluoride concentration on adsorption by GO. Results shows that the adsorption decreases with increase in the concentration of fluoride by GO. Babaeivelni et al. (2013) has also reported, the decrease in adsorption with increase in the fluoride concentration, as an effect of saturation of all available sites for adsorption.

Figure 10 Fluoride removal (%) at different adsorbent doses (100–250 mg/l) (see online version for colours)

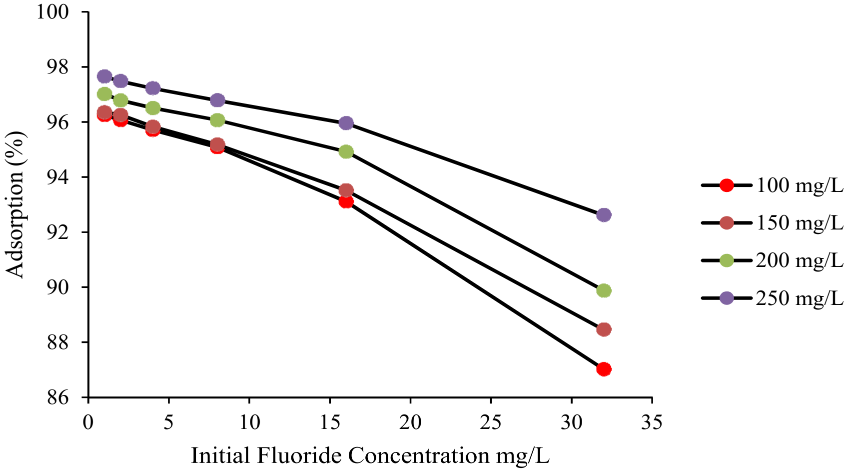

12 Adsorbent doses

Adsorption efficiency of adsorbent was tested with varying fluoride concentrations (1–32 mg/L). Figure 11 show the effect of adsorbent (GO) mass on the amount of fluoride removal. The different adsorbent dose from 100–250 mg/L to 1–32 mg/L of fluoride concentration were applied. The increasing adsorbent mass from 100–250 mg/L results in significant increase in adsorption. The optimum fluoride removal 98% was observed at 250 mg/L of adsorbent dose to 32 mg/L of fluoride.

Figure 11 Effect of adsorbent (GO) on fluoride removal (%) at pH 6 (see online version for colours)

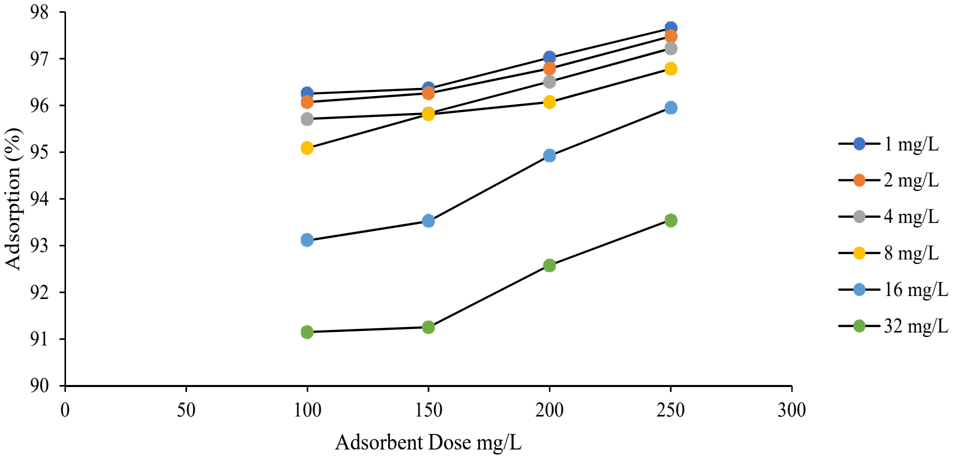

The maximum adsorbent dose provides plenty of binding sites for adsorption and hence, increased removal (Fufa et al., 2013; Gupta et al., 1997).

13 Effect of variation in temperature on fluoride adsorption

The effect of temperature on fluoride adsorption was analysed at three different (298 K, 308 K and 318 K) temperatures and constant experimental conditions. The temperature is an important parameter for adsorption of F^- on GO surface (Bajpai et al., 2017). The fluoride removal process at equilibrium, the adsorption capacity of adsorbent changes with increase in temperature and the maximum adsorption 97.65 % was reached at 298 K. Adsorption efficiency was decreased with increasing temperature, this indicates the fluoride adsorption is a exothermic process (Figure 12) (Tirkey et al., 2017; Gupta et al., 2016). The low temperature facilitates the chemisorption process at 298 K. The removal efficiency was found decreased at higher temperatures, i.e., 308 K and 318 K.

Figure 12 Effect of variation in temperature on fluoride removal (see online version for colours)

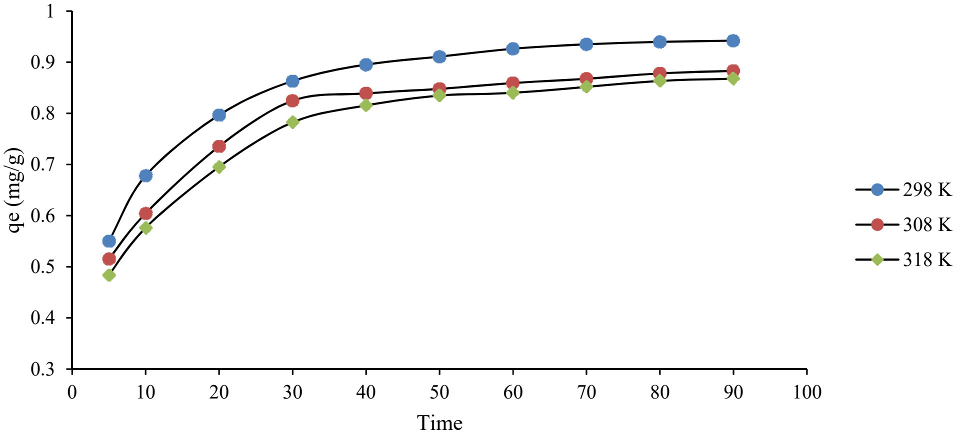

Note: Fluoride concentration 2 mg/l and GO dose 100 mg/l at pH 6.

14 Kinetics studies

In order to determine the efficiency of the adsorbent and the mechanism of the adsorption four models, pseudo-first-order [equation (4)], pseudo-second-order [equation (5)], intraparticle diffusion model [equation (6)] and Elovich model [equation (7)] were applied. Different parameters were used to plot the kinetic model and concise it with coefficients in Table 1. The equation for kinetic models is as follows.

- Pseudo-first-order equation:

$$\log\left(q_e - q_t\right) = \log q_e - \left(K_f / 2.303\right)t \tag{4}$$

- Pseudo-second-order equation:

$$t / qt = 1 / Ksq_e^2 + \left(\frac{1}{q_e}\right)t \tag{5}$$

where q_e is the adsorption capacity at equilibrium (mg/g), qt is the adsorbed amount of fluoride (mg/g) at time t, and K_f is the constant rate of pseudo-first-order and Ks is the constant rate of pseudo-second-order (mg min –1) (Jethave et al., 2018; Mohammadi et al., 2011). The graph plotted by using values intercept $\log\left(q_e - q_t\right)$ vs. t (Figure 12). Five initial concentration of fluoride (1, 2, 4, 8, 16 and 32 mg/L) was considered for kinetic study. The linearity of the pseudo-second-order kinetic model with correlation coefficient (R^2 0.995), clearly reveals the chemisorption is involved in the fluoride removal.

The Weber and Morris proposed the Intra-particle diffusion model equation [equation (6)] for kinetic study. Usually, the intraparticle diffusion is based on the initial concentration of the solution, physical properties of adsorbent, and temperature. The adsorption of fluoride ions on the GO surface can be explained with intraparticle diffusion model. Geethamani et al. (2014) reported that the adsorption is almost proportionate to the $t^{1/2}$ functionality relationship with intraparticle diffusion treatment (Nekouei et al., 2015; Saleh and Gupta 2012a). The intraparticle diffusion equation is as follow:

$$q_t = K_{id} t^{1/2} + C \tag{6}$$

where, *qt* amount of fluoride adsorbed, K_{id} is the rate constant of intra-particle diffusion and *C* is the intercept (Alien et al., 2018; Saleh and Gupta 2014). The intermittent batch adsorption process for the mass transfer of fluoride ions is only applicable at the higher fluoride concentration, i.e., >16 mg/L.

Figure 13 Pseudo-second-order kinetics for fluoride removal by GO (see online version for colours)

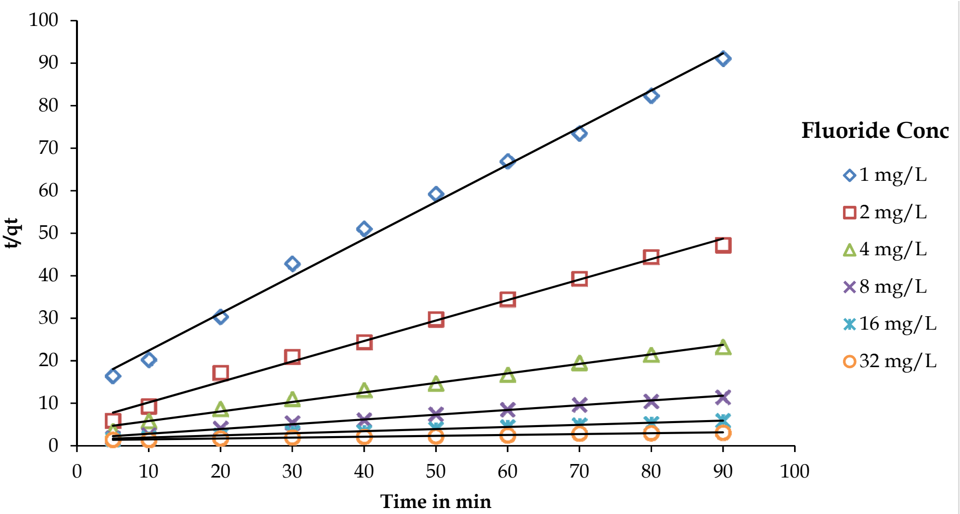

Note: 250 mg/l adsorbent concentration, temp 298 K and pH 6.

The Elovich equation was described by Zeldowitsch in 1934. The adsorption process using different adsorbent molecules from contaminate present on liquid media was determined by Elovich equation [equation (7)], it describe the adsorption rate of fluoride on graphene oxide.

$$q_t = \left(\frac{1}{\beta In(\alpha\beta)} + \frac{1}{\beta} \right) In\ t \tag{7}$$

where q_t represent the adsorbed amount of fluoride at time t, α is the constant desorption, and β is the rate of initial adsorption. The plot of *qt* versus *Int*, with a slope and intercept of $(1/\beta)$ and $(1/\beta)\ In(\alpha\beta)$, respectively (Ayari et al., 2009). The results indicates that the fluoride adsorption process on GO surface do not obey the Elovich model.

Table 1 Kinetic parameter of fluoride onto GO

Models	*Parameters*	*Initial fluoride concentration (mg/L)*					
		1	*2*	*4*	*8*	*16*	*32*
First order kinetic	$k_f \times 10^2$	1.887	3.777	3.382	2.724	3.218	2.466
	Qe	2.5787	2.397	1.706	1.121	3.31	4.519
	R^2	0.9473	0.829	0.901	0.893	0.863	0.897
Second order kinetic	K^2	25.43	1.088	0.321	0.0915	0.0445	0.0144
	Qe	1.144	9.049	4.518	2.095	19.564	36.363
	R^2	0.9947	0.9929	0.9922	0.9946	0.9912	0.9936
Intra-particle diffusion	Kid1	0.085	1.289	0.177	0.354	1.58	2.585
	C	0.2305	1.421	0.441	0.636	0.522	1.852
	R^2	0.9583	0.959	0.9284	0.987	0.994	0.993
	Kid^2	0.0607	0.4868	0.084	0.177	1.035	4.24
	c	0.4252	3.224	1.078	2.158	5.53	1.064
	R^2	0.9526	0.992	0.9337	0.936	0.944	0.946
Elovich	α	0.236	2.32	1.2	0.595	10.3777	18.34
	β	4.746	0.555	1.111	2.654	0.241	0.138
	R^2	0.9753	0.9796	0.964	0.9536	0.963	0.902

Note: Adsorbent dose 250 mg/L and initial fluoride conc. 1–32 mg/L.

15 Adsorption isotherm study

The correlation of equilibrium curves is important and appropriate to establish the optimisation of the adsorption process of the contaminants (Rajendra et al., 2016; Saravanan et al., 2013b; Ali, 2012). As expected optimum adsorption efficiency of adsorbent under a given condition, by which removal efficiency of GO depends on the equilibrium curve recognised in between adsorbed sites of adsorbent and fluoride concentration. The GO adsorption capacity (adsorbent curve) investigated using isotherm of F^- by GO with given experimental condition like contact time, pH, adsorbent dose and temperature. These parameters are must for isotherm model to fit the experimental data to obtain the correlation curve of the soluble concentration in the solid state. Experimental data were analysed using isotherm models such as Langmuir, Freundlich, Temkin, Dubinnin-Radushkevich (D-R) and Harkins-Jura (H-J).

The Langmuir model determines the nature of adsorption and amount of fluoride removed by GO.

The Longmuir equation is stated as:

$$\frac{C_e}{q_e} = \frac{Ce\alpha_L}{K_L} + \frac{1}{K_L} \tag{8}$$

where $Qm = a_L/K_L$ (mg/g) represents maximum adsorption capacity of the adsorbent, q_e is the equilibrium of adsorbent adsorbed per unit of adsorbate (mg/g), C_e represents aqueous-phase adsorbate concentration (mg/L) and KL Langmuir constant (L/mg). A plot of *Ce*/*qe* versus *Ce* at different amount of GO in the range of 100–250 mg should shows a straight line with slope of *Qm* and intercept is equal to $1/K_L$ by comparing the correlation coefficients of isotherm models of experimental data (Jethave et al., 2018; Suhas et al., 2016; Saravanan et al., 2013c). The Langmuir isotherm model curve can be seen in Figure 14. The experimental data linearly obeys the Langmuir isotherm and indicates the monolayer adsorption with 18.86 mg/g of fluoride removal capacity.

Figure 14 Intra-particle diffusion model of fluoride removal onto GO: fluoride concentration 2 mg/l, at pH 6.0 (see online version for colours)

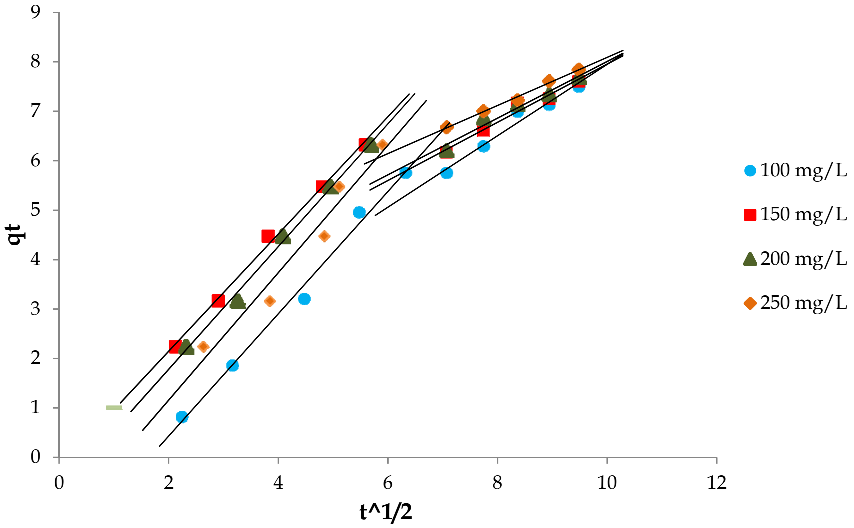

The adsorption of fluoride can be described by the commonly used isotherm models. The Freundlich equation is often useful for modelling fluoride onto solids with heterogeneous surfaces and has frequently proved superior to the Langmuir equation for the adsorption of cations such as fluoride. Freundlich constant related to the distribution coefficient (kF), are widely acceptable in characterising the fluoride adsorption capacity. (Alsulaili and Fahim 2020; Ghaedi et al., 2015; Gupta et al., 2013)

$$InQe = \frac{1}{InCe} + Ink_f \tag{9}$$

where, Q_e for the amount of fluoride adsorption at equilibrium (mg/g), were k_f Freundlich constant indicate the adsorption efficiency and adsorption intensity respectively [equation (9)] (Ghosh et al., 2016; Singh et al., 2017; Saravanan et al., 2016). Freundlich equation, suggests heterogeneous adsorption on the uneven surface and the concentration of adsorbate adsorbed increases with increasing adsorbent dose (Adekola et al., 2020; Araghia and Entezari et al., 2015; Saravanan et al., 2015). Table 2 shows, k_f and n the Freundlich parameter, related to the affinity of the adsorbate and fluoride adsorption intensity respectively. The K_f and *n* values can be determined by intercept and slope of the linear plot of *Inqe* versus *InCe* (Zhou et al., 2019; Saravana et al., 2013d; Saleh et al., 2012b). The *n* values calculated from experiment data of fluoride adsorption shows that the Freundlich isotherm is favourable for fluoride adsorption on GO.

$$q_e = B_1\ In\ KT + B_1\ InsC_e \tag{10}$$

It is expected in the Temkin isotherm model that the heat of adsorption should decrease linearly with coverage of GO surface. The fluoride adsorption on the GO is an exothermic process and do not obey the Temkin isotherm. Where, *KT* is the equilibrium binding constant (L/mg), *T* indicates the temperature in *K* and B_1 is related to adsorption of heat [equation (10)] (Jethave et al., 2018; Adrian et al., 2017; Saravanan et al., 2013e). Table 2 shows the Temkin isotherm constant, the B1 values changed from 0.242 to 1.389 with increasing adsorbent dose (100–250 mg).

Table 2 Isotherm constant for adsorption of fluoride by GO

Isotherm	*Linear form*	*Parameters*	*Adsorbent doses (mg/L)*			
			100	*150*	*200*	*250*
Langmuir	*Ce/qe* = *CeαL*/*KL* +1/*KL*	q_m (mg/g)	18.86	13.29	10.00	8.63
		KL (L/mg)	12.37	8.59	7.81	7.80
		R^2	0.996	0.995	0.998	0.995
Freundlich	*lnQe* = 1/*n* *1nCe*+ln*kf*	n	1.38	1.35	1.35	1.33
		K_f (L/mg)	6.15	4.38	3.77	3.72
		R^2	0.982	0.986	0.982	0.984
Temkin	*qe* = *B*1 l*n KT* + *B*1 l*n Ce*	B1	0.242	2.540	1.876	1.389
		KT (L/mg)	10.88	7.205	9.543	19.40
		R^2	0.915	0.913	0.923	0.925
Dubinin-Radushkevich (DR)	*lnqe* = *lnQs* – *Bε*2	Qs (mg/g)	15.67	5.906	4.671	3.996
		B	0.006	0.00008	0.00007	0.00004
		E (kj/mol)	28.86	790	845	1118
		R^2	0.981	0.880	0.896	0.908
Harkins–Jura (H-J)	1/Qe^2 = [*B*/*A*]- [1/*A*] *logCe*	A	1.47	0.674	0.408	0.310
		B	0.299	0.239	0.162	0.023
		R^2	0.660	0.661	0.649	0.651

Dubinin-Radushkevich (D-R) isotherm models are widely used by environmentalists to optimise a design of the adsorption system. In the present study, the adsorption of fluoride onto the adsorbents (GO) was studied at different temperatures (298 K, 308 K and 318 K) and the applicability of the above isotherms was examined (Kacho et al., 2020; Gupta et al., 2014b; Mittal et al., 2010).

$$q_e = q_{max} exp\left(-B\varepsilon^2\right) \tag{11}$$

$$Inq_e = InQ_s - B\varepsilon^2 \tag{12}$$

where, Q_{max} is constant of D-R (mg/g), *B* is the energy adsorption constant, *ε* represents the Polanyi potential, calculated from equation (12). The Dubinin-Radushkevich (D-R) isotherm model considers that adsorbent size and adsorption equilibrium related to given fluoride-GO combination can be stated separately of temperature by using adsorption potential conferring to equation (13) (Selvan and Sundari, 2020; Ghadim et al., 2013).

The Harkins-Jura (H-J) adsorption isotherm stated as below:

$$\frac{1}{Qe^2} = \left[\frac{B}{A}\right] - \frac{1}{A} logCe \tag{13}$$

where, the adsorption of fluoride by GO is q_e (mg/g), the concentration of equilibrium is *Ce* (mg/L), isotherm constant are *A* and *B*. The *A* and *B* values calculated from the plot of 1/*qe*2 versus *logCe* [equation (13)]. Table 2 shows the calculated values. The results in Table 2 indicates that the adsorption of fluoride on the surface of GO surface follows monolayer adsorption. By comparing the coefficient R^2 values of the examined four isotherm models, it can be concluded that the Langmuir models fit the experimental data. The Langmuir and Freundlich models gave better fit than the D-R and H-R isotherm models. The optimum fluoride removal capacity as per the Langmuir isotherm model is 18.86 mg/g.

16 Separation factor

The separation factor R_L, were calculated from Langmuir isotherm constant K_L and the initial concentration of fluoride is *Co*, was used to investigate the attraction between the $F^-$and GO in aqueous solution. The dimensionless constant separation factor R_L expressed in equation (14) (Melidis, 2015).

$$R = \left(\frac{1}{1+\alpha_L\ C_o}\right) \tag{14}$$

The Langmuir isotherm indicates:

If reversible $R_L = 0$,
Linear $R_L = 1$,
Unfavourable if $R_L > 1$
Favourable if $0 < R_L < 1$

Figure 15 Langmuir isotherm model for four different adsorbents (GO) doses (100–250 mg/l) (see online version for colours)

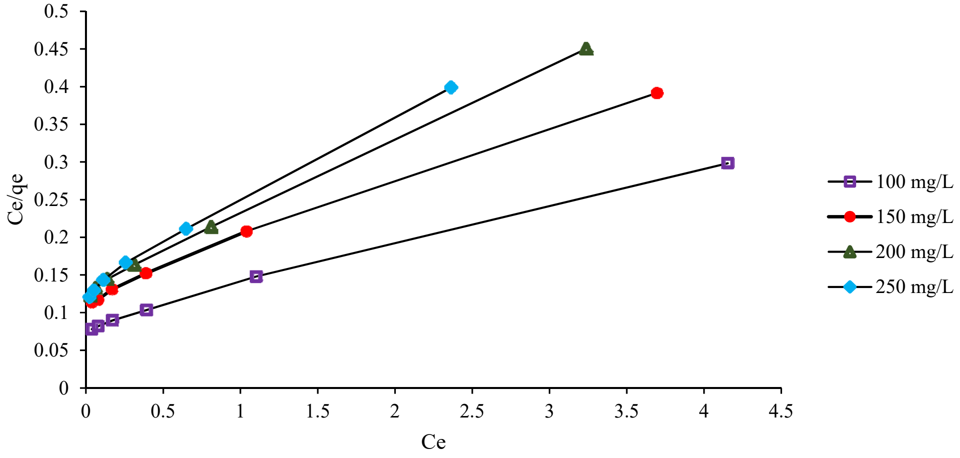

Figure 15 shows the RL values 0.49 to 0.77 indicates the adsorption is favourable. These results reveal that GO has a monolayer adsorption (Geethamani et al., 2014).

Figure 16 Separation factor of defluoridation onto GO (see online version for colours)

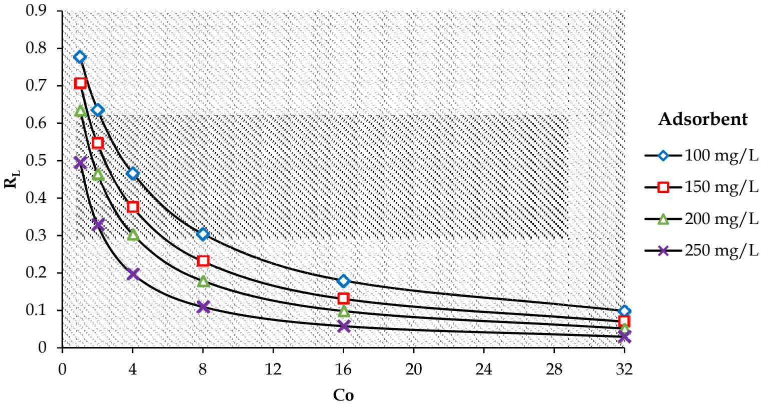

17 Thermodynamic studies

The thermodynamic study is essential for solid-liquid adsorption process. In this study effect of temperature on adsorption is investigated in the rage of 298–318 K. The experimental parameter such as adsorbent dose, contact time and solution pH were kept fixed at 100–250 mg/L, 90 min and pH 6 respectively. The results showed that fluoride adsorption capacity decreases with increasing temperature. Adsorption thermodynamics is calculated using Gibbs free energy change (ΔG^o), standard enthalpy change (ΔH^o), and standard entropy (ΔS^o) (Devraj et al., 2016; Gupta et al., 2014c)

$$InK_c = \frac{\Delta S^o}{R} - \frac{\Delta H^o}{RT} \tag{15}$$

$$\Delta G^o = RTInK_c \tag{16}$$

$$K_c = \frac{q_e}{C_e} \tag{17}$$

where R is the universal gas constant, T is the temperature (in Kelvin), K_c is the constant thermodynamic equilibrium. The results reveal that the –5.29, –5.79 and –6.25 kJ/mol for 298 K, 308 K and 318 K are the ΔG° values of the adsorption, respectively (Table 3). According to negative values of adsorption ΔG°, reveals the feasibility and spontaneity of the adsorption process in the given temperature are favourable for 298 K temperature. The negative values of ΔH° (–0.0074 kJ/mol) indicate the process of adsorption is exothermic nature due to the ion exchange reaction on the GO surface (Li et al., 2011).

Table 3 Adsorption thermodynamic of defluoridation by GO

ΔH° (kJ/mol)	*ΔS° (J/mol)*	*ΔG°(kJ/mol)*		
		298 ^{0}K	*308 ^{0}K*	*318 ^{0}K*
–0.0074	–0.044	–5.29	–5.78	–6.25

18 Reusability study

Reusability is one of the most important aspects that should be considered in cost-effective adsorbent (Pourbeyram, 2019; Khani et al., 2010). The reusability of GO was determined for reabsorption of fluoride. To test the reuse of adsorbent, the adsorption cycle was repeated five times, using the same adsorbent without desorption of fluoride. The result of five reuse cycles are shown in Figure 17. The result indicates that the fluoride removal percentage decreases with the number of increase in cycles. The fluoride adsorption in fist cycle is 98.6% and the fifth cycle is was 63.99%. These results indicate good adsorption performance up to 3rd cycle.

Figure 17 Reusability study of the GO for fluoride adsorption (see online version for colours)

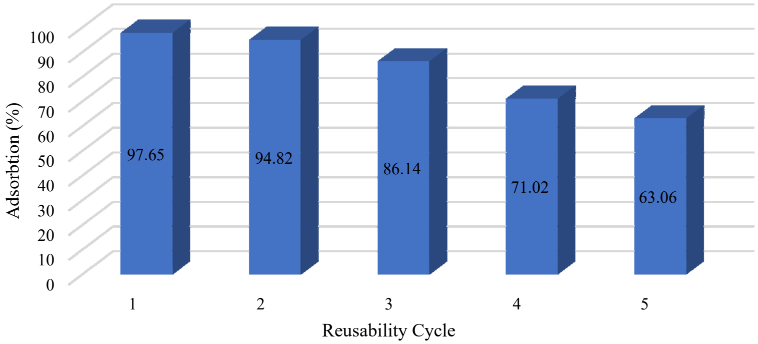

Note: Fluoride concentration 2 mg/l, adsorbent dose 100 mg/l at pH 6.

19 Anion interference and fluoride adsorption

The fluoride adsorption experiments, and the study was done with synthetic fluoride water. It is very necessary to take into account the interference of the other cation and anions present in the water. The effect of individual anions (Cl^-, SO^-_4–, NO^-_3–, F^-) was studied through FTIR analysis. In order to understand the mechanism and interference of other ionic species, a real water sample from a fluorite mine located in Nagpur district was collected, treated with GO and analysed.

Figure 18 shows the FTIR spectrum of different anions behaviour with graphene oxide. In order to understand the exact interaction between anions and graphene oxide, the salt solutions of sodium chloride (green) (100 mg/L), sodium sulphate (red) (100 mg/L), and sodium nitrate (blue) (100 mg/L), were shaken separately with graphene oxide, and after treatment FTIR scan was performed. The GO (green) shows a strong doublet peak at 2,359 cm^{-1} and 2,342 cm^{-1}, this is a clear indication that the carbonyl group of the GO make a bond with chloride ion -C-O-Cl, this bond formation creates a strong dipole moment and the peaks are evident in the FTIR analysis, on the other hand –SO^{-}_{4}–, –NO^{-}_{3}–, and –F^{-} are not interfering with the carbonyl oxygen. The peaks are again confirmed the -C-O-Cl bonding on the GO after treating the fluorite mining sample water (dark red). The fluoride adsorption is mainly governed by the ion exchange process at the hydroxyl group -OH- as it is replaced by fluoride ion, the evident peaks of the hydroxyl group on GO at 3,634 cm^{-1} is reduced in fluoride-containing samples (violet and dark red). The sulphate ions having electrostatic interactions with the carbonyl and hydroxyl group, it is confirmed by the vibrational multi-peaks in 4,000–3,500, and 1,764–1,435 cm^{-1} region. The nitrate does not show any characteristic changes in the GO FTIR scan, however, the adsorption of nitrate was 69.22%, and this may be a surface complexation between C-pi electron of GO sheets and the nitrate ions.

Figure 18 Anions interaction with graphene oxide (see online version for colours)

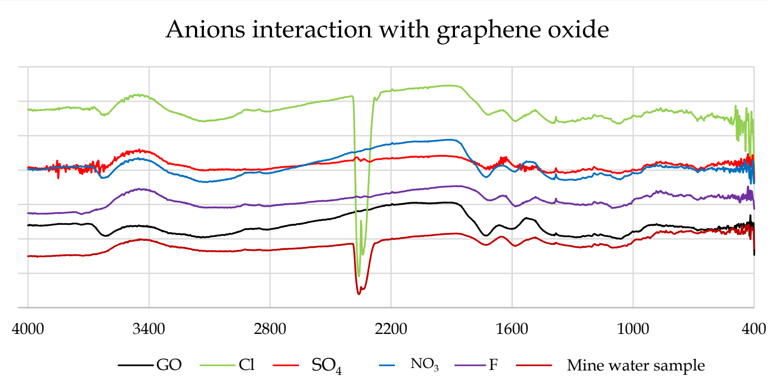

Table 4 Fluorite mine water sample before and after treatment with graphene oxide

Parameter	*Before treatment*	*After treatment*
pH	6.9	6.8
EC (mS/cm)	122.33	64.13
TDS (mg/L)	622.5	204.66
Sulphate (mg/L)	284.26	80.23
Nitrate (mg/L)	60.66	17.16
Phosphate (mg/L)	BDL	BDL
Chloride (mg/L)	136.5	56.33
Fluoride (mg/L)	17.1	BDL

Notes: Adsorbent dose 250 mg/L. BDL – below the limit.

In order to assess the applicability of the GO for the real water samples and to check the interference effect of the other anions, the real water sample was treated with the graphene oxide, as the results can be seen in Table 4, the overall efficiency of the GO is much more than the qmax obtained for fluoride only. The interference of the other anions are found negligible on the fluoride adsorption.

Table 5 Comparison with various adsorbents

Adsorbents	*Dosage (g/L)*	*Time*	*pH*	*T (°C)*	*Fluoride concentration (mg/L)*	q_{max} *(mg/g)*	*Ref.*
Y-GO-SA1.0	0.01	24 hr	4	-	10–200	288.96	He et al. (2018)
lAO/GO	0.25	20 hrs	6.5	25	2–50	64.72	Liu et al. (2016a)
Al-La@CG	0. 5	400 min	4	25	5–100	51.54	Guo et al. (2019)
GO-Al-O(OH)	0.5	24 hrs	7	20	1–5	51.41	Barathi et al. (2014)
lAO	0.25	20 hrs	6.5	25	2–50	46.54	Liu et al. (2016a)
Zr-La-CC/GO	0.5	400 min	7	40	1 - 100	38.80	Shang et al. (2019)
β-FeOOH@GO	0.05	8 hrs	7–8	25	1–25	17.67	Liu et al. (2016b)
FeOOH-GO	2.5	8 h	7	25	10–150	17.65	Kuang et al. (2017)
GO/Al2O3	4.0	60 min	6	25	1–20	11.52	Xu et al. (2020)
Ox-GO-Zr	0.01	20 min	7	25	1–10	8.76	Prabhu et al. (2016)
GOAlgLa	2.0	70 min	3	30	1–20	6.70	Pandi et al. (2016)
Zr-Ox	0.01	20 min	7	25	1 –10	5.97	Prabhu et al. (2016)
Graphene-ZrCl4/VAC	0.1	5 hrs	5.5	30	1–15	3.87	Marin et al. (2016)
Al2O3-Fe2O4/EG	0.2	120 min	4	30	1–20	3.35	Xu et al. (2016)
Activated carbon	0.15	100 min	4	30	2–8	2.52	Bhomick et al. (2019)
GO	0.25	30 min	6	25	1–32	18.86	Present study

To understand the characteristic and designing of the adsorbent for water purification, the mechanism of adsorption phenomenon is important. Thus, considering the experimental results and investigation of mathematical models for the adsorption mechanism of fluoride by GO can be proposed. As the adsorption of fluoride ion on GO is chemisorption. At pH 6 the GO sheet gets positive charge and the hydroxyl ion on the edges of the GO are exchanged by the fluoride ions, the fluoride adsorption by GO is governed by chemisorption was further supported by the values of pseudo second order and thermodynamic parameter investigated in the study. The mechanism ratifies that the adsorption of fluoride is a function of the hydroxyl groups available on GO.

The comparison shows yttrium-graphene composite is having better fluoride removal efficiency than the GO but the time required for adsorption is more (Table 4). Moreover, rare earth metals and precious metal shows optimum fluoride removal ability, but the low abundance make its use hardly possible. The GO is superior than other adsorbents for its higher adsorption capacity with respect to adsorbent dose and time required for fluoride removal and not only fluoride but chloride is also adsorbed very well on it.

20 Conclusions

The GO was synthesised by modified Hummer's method and the surface characteristic, crystallographic structure and functional groups present were studied. The synthesised GO was used as an adsorbent for fluoride removal from the water. This research work demonstrated that the GO exhibits a good adsorption ability for the defluoridation of water. The active functional groups on the large surface area of GO have facilitated high adsorption of fluoride. Adsorption kinetic data best fitted in the pseudo-second-order model which reveals that fluoride removal is a chemisorption process. Maximum fluoride adsorption capacity of GO calculated by the Langmuir isotherm model is 18.86 mg/g. The maximum fluoride removal was achieved at 27.84 mg/L at 298 K in acidic condition at pH 6. As compared to the other adsorbent used for adsorption of fluoride verified in the literature, GO shown appreciable adsorption capacity within minimum time period and less quantity of adsorbent. The thermodynamic study illustrated the adsorption is an exothermic reaction. The reusability was successfully done at 86% removal up to 3rd cycle. Overall, GO is a trusted adsorbent for fluoride removal and may even apply to actual fluoride contaminated water samples.

Acknowledgements

One of the authors, Mr. Ram A. Konale sincerely acknowledges the fellowship provided under DST INSPIRE, Scheme by Department of Science and Technology, Government of India (DST/INSPIRE Fellowship/[IF170674]).

References

Adekola, F., Adegoke, H., Arowosaiye, O. and Olatunji, G. (2020) 'Kinetic and thermodynamic studies of sorption of lead and cadmium from aqueous solution by Moringa oleifera pod wastes', *International Journal of Environment and Waste Management*, Vol. 25, No. 1. pp.58–82.

Adrian, B.P., Didilia, I.M. and Hilda, E.R. (2017) *In Adsorption Processes for Water Treatment and Purification*, Springer, New York, USA.

Ahmaruzzaman, M. and Gupta, V.K. (2011) 'Rice husk and its ash as low-cost adsorbents in water and wastewater treatment', *Industrial and Engineering Chemistry Research*, Vol. 50, No. 24, pp.13589–13613.

Alexander, E.B., Evgeny, V.G., Irina, V.B., Anastassia, E.K., Agarwal, S., Alexey, G.T. and Gupta, V.K. (2018) 'Adsorption of heavy metals on conventional and nanostructured materials for wastewater treatment purposes: a review', *Ecotoxicology and Environmental Safety*, Vol. 148, No. 22, pp.702–712.

Ali, I. (2012) 'New generation adsorbents for water treatment', *Chemical Reviews*, Vol. 112, No. 10, pp.5073–5091.

Alien, B.F., Nubia, A.L., Victor, P.G., Jose, M.G., Maria, O.E. and Israel, R.T. (2018) 'Efficient fluoride removal using Al-Cu oxide nanoparticles supported on steel slag industrial waste solid', *Environmental Science and Pollution Research*, Vol. 25, No. 7, pp.6414–6428.

Alipanahpour, D.E., Ghaedi, M., Ghaedi, A.M., Asfaram, A., Goudarzi, A., Hajati, S., Soylak, M., Agarwal, S. and Gupta, V.K. (2015) 'Modeling of quaternary dyes adsorption onto ZnO-NR-AC artificial 3 neural network: analysis by derivative spectrophotometry', *Journal of Industrial and Engineering Chemistry*, Vol. 34, pp.186–197.

Alsulaili, A.D. and Fahim, A.M. (2020) 'Oil removal from produced water by agriculture waste adsorbents', *International Journal of Environment and Waste Management*, Vol. 25, No. 1, pp.12–31.

APHA, AWWA and WEF (1996) *Standard Methods for the Examination of Water and Wastewater*, 19th ed., p.657, Washington, DC.

Araghia S.H. and Entezari, M.H. (2015) 'Amino-functionalized silica magnetite nanoparticles for the simultaneous removal of pollutants from aqueous solution', *Journal of Applied Surface Science*, Vol. 333, pp.68–77.

Asfaram, A., Ghaedi, M., Agarwal, S., Tyagib, I. and Gupta, V.K. (2016) 'Removal of basic dye Auramine-O by ZnS: cu nanoparticles loaded on activated carbon optimization of parameters using response surface methodology with central composite design', *RSC Advances*, Vol. 5, pp.18438–18450.

Athanasia, K.T., Mitrakas, M., Katsoyiannis, I.A., Ernst, M. and Zouboulis, A.I. (2019) 'Fluoride removal from water by composite Al/Fe/Si/Mg pre-polymerized coagulants: characterization and application', *Chemospere*, *CHEM*, DOI: 23918.

Augustine, M. and Pius, A. (2017) 'Removal of fluoride from drinking water using aluminum hydroxide coated activated carbon prepared from bark of Morinda tinctoria', *Applied Water Science*, Vol. 7, pp.2653–2665.

Ayari, F., Srasra, E. and Trabelsi-Ayadi, M. (2009) 'Low-cost adsorbents for a dye uptake from contaminated water modeling of adsorption isotherms: the Langmuir, Freundlich and Elovich models', *Electrical Processes in Engineering and Chemistry*, Vol. 44, pp.489–498.

Babaeivelni, K. and Khodadoust, A.P. (2013) 'Adsorption of fluoride onto crystalline titanium dioxide: Effect of pH, ionic strength, and co-existing ions', *Journal of Colloid and Interface Science*, Vol. 394, No. 15, pp.419–427.

Bajpai, A.K., Dubey, R. and Bajpai, J. (2017) 'Synthesis, characterization, and adsorption properties of a graphene composite sand (GCS) and its application in remediation of Hg(II) ions', *Water Air Soil Pollut*, Vol. 228, No. 9, p.346.

Barathi, M., Krishna, K.A., Uday, K.C. and Rajesh, N. (2014) 'Graphene oxide-aluminium oxyhydroxide interaction and its application for the effective adsorption of fluoride', *RSC Advances*, Vol. 4, No. 96, pp.53711–53721.

Bhaumik, R. and Mondal, N. (2015) 'Adsorption of fluoride from aqueous solution by a new low-cost adsorbent: thermally and chemically activated coconut fibre dust', *Clean Technologies and Environmental Policy*, Vol. 17, pp.2157–2172.

Bhomick, P.C., Supong, A., Karmaker, R., Baruh, M., Pongener, C. and Sinha, D. (2019) 'Activated carbon synthesized from biomass material using single-step KOH activation for adsorption of fluoride: experimental and theoretical investigation', *Korean Journal of Chemical Engineering*, Vol. 36, pp.551–562.

Biswas, G., Kumari, M. and Adhikari, K. (2017) 'A critical review on occurrence of fluoride and its removal through adsorption with an emphasis on natural minerals', *Water Pollution*, Vol. 3, No. 2, pp.104–119.

Chiavola, A., Amato, E.D. and Boni, M.R. (2019) 'Comparison of different iron oxide adsorbents for combined arsenic, vanadium and fluoride removal from drinking water', *International Journal of Environmental Science and Technology*, Vol. 16, pp.6053–664.

Corral, N.G., Vilchis, A.R., Gutierrez, E. and Solache, M. (2019) 'Comparison of the removal behavior of fluoride by Fe3+ modified geomaterials from water', *Applied Clay Science*, Vol. 173, pp.19–28.

Dehghani, M.H., Farhang, M., Alimohammadi, M., Afsharnia, M. and Mckay, G. (2018) 'Adsorptive removal of fluoride from water by activated carbon derived from CaCl2-modified crocus sativus leaves: equilibrium adsorption isotherms, optimization, and influence of anions', *Chemical Engineering Communications*, Vol. 205, No. 7, pp.955–965.

Devaraj, M., Saravanan, R., Deivasigamani, R., Gupta, V.K., Gracia, F. and Jayadevan, S. (2016) 'Preparation of novel shape Cu and Cu/Cu_2O nanoparticles for the determination of dopamine and paracetamol', *Journal of Molecular Liquids*, Vol. 221, pp.930–941.

Dhillon, A., Nehra, S., Choudhar, B.L., Kumar, D. and Prasad, S. (2017) 'Excellent disinfection and fluoride removal using bifunctional nanocomposite', *Chemical Engineering Journal*, Vol. 377, pp.193–200.

Duraiswami, R. and Patankar, U. (2011) 'Occurrence of fluoride in the drinking water sources from Gad river basin, Maharashtra', *Journal Geological Society of India*, Vol. 77, pp.167–174.

Esmeralda, V., Jose, L.F., Horacio, F. and Jose, R. (2019) 'Fluoride removal from water by ceramic oxides from cerium and manganese solutions', *Journal of Molecular Liquids*, Vol. 286, p.110880.

Ezzeddine, A., Bedoui, A., Hannachi, A. and Bensalah, N. (2014) 'Removal of fluoride from aluminum fluoride manufacturing wastewater by precipitation and adsorption processes', *Desalination and Water Treatment*, Vol. 54, No. 8, pp.2280–2292.

Fufa, F., Alemayehu, E. and Lennartz, B. (2013) 'Defluoridation of groundwater using termite mound', *Water, Air, and Soil Pollution*, Vol. 224, No. 5, pp.1–15.

Geethamani, C.K., Ramesh, S.T., Gandhimathi, R. and Nidheesh, P.V. (2014) 'Alkali-treated fly ash for the removal of fluoride from aqueous solutions', *Desalination and Water Treatment*, Vol. 52, Nos. 19–21, pp.3466–3476.

Ghadim, E.E., Manouchehri, F., Soleimani, G., Hosseini, H., Kimiagar, S. and Nafisi, S. (2013) 'Adsorption properties of tetracycline onto graphene oxide: equilibrium, kinetic and thermodynamic studies', *PLOS One*, Vol. 8, No. 11, p.e79254.

Ghaedi, M., Hajjati, S., Mahmudi, Z., Tyagi, I., Agarwal, S., Maity, A. and Gupta, V.K. (2015) 'Modeling of competitive ultrasonic assisted removal of the dyes – methylene blue and Safranin-O using Fe_3O_4 nanoparticles', *Chemical Engineering Journal*, Vol. 268, pp.28–37.

Ghosh, S.B., Bhaumik, R. and Mondal, N.K. (2016) 'Optimization study of adsorption parameters for removal of fluoride using aluminium-impregnated potato plant ash by response surface methodology', *Clean Technologies and Environmental Policy*, Vol. 18, No. 4, pp.1069–1083.

Gogoi, C., Saikia, J., Sarmah, S., Sinha, D., Goswamee, R.L. (2018) 'Removal of fluoride from water by locally available sand modified with a coating of iron oxides', *Water, Air, Soil Pollution*, Vol. 229, No. 4, p.118.

Guo, Y., Xu, X., Shang, Y., Gao, B., Zhang, L., Yue, Q., Li, Q. and Wang, Z. (2019) 'Multiple bimetallic (Al-La or Fe-La) hydroxides embedded in cellulose/graphene hybrids for uptake of fluoride with phosphate surroundings', *Journal of Hazardous Materials*, Vol. 379, DOI: 120634.

Gupta, V.K., Ali, I., Saleh, T.A., Siddiqui, M.N. and Agarwal, S. (2013) 'Chromium removal from water by activated carbon developed from waste rubber tires', *Environmental Science and Pollution Research*, Vol. 20, pp.1261–1268.

Gupta, V.K., Atar, N., Lütfi, M., Ustundag, Z. and Uzun, L. (2014) 'A novel magnetic Fe@Au core-shell nanoparticles anchored graphene oxide recyclable nanocatalyst for the reduction of nitrophenol compounds', *Water Research*, Vol. 48, No. 1, pp.210–217.

Gupta, V.K., Bhanu, P., Pathania, D. and Singh, A.S. (2014) 'Synthesis, characterization and antibacterial activity of biodegradable Starch/PVA composite films reinforced with cellulosic fibre, *Carbohydrate Polymers*, Vol. 109, pp.171–179.

Gupta, V.K., Jain, C.K., Ali, I., Chandra, S. and Agarwal, S. (2002) 'Removal of lindane and malathion from wastewater using bagasse fly ash-a sugar industry waste', *Water Research*, Vol. 36, No. 10, pp.2483–2490.

Gupta, V.K., Jain, R., Nayak, A., Agarwal, S. and Shrivastava, M. (2011) Removal of the hazardous dye-Tartrazine by photodegradation on titanium dioxide surface', *Material Science and Engineering C*, Vol. 31, No. 5, pp.1062–1067.

Gupta, V.K., Nayak, A. and Agarwal, S. (2015) 'Bioadsorbents for remediation of heavy metals: current status and their future prospects', *Environmental Engineering Research*, Vol. 20, No. 1, pp.1–18.

Gupta, V.K., Nayak, A., Agarwal, S. and Tyagi, I. (2014) 'Potential of activated carbon from Waste Rubber Tire for the adsorption of phenolics: effect of pre-treatment conditions', *Journal of Colloid and Interface Science*, Vol. 417, pp.420–430.

Gupta, V.K., Rastogi, A., Dwivedi, M.K. and Mohan, D. (1997) 'Process development for the removal of zinc and cadmium from wastewater using slag-a blast furnace waste material, *Separation Science and Technology*, Vol. 32, No. 17, pp.2883–2912.

Gupta, V.K., Tyagi, S.I., Agarwal, S., Singh, R., Chaudhary, M., Harit, A. and Kushwaha, S. (2016) 'Column operation studies for the removal of dyes and phenols using a low-cost adsorbent', *Global Journal of Environmental Science Management*, Vol. 2, No. 1, pp.1–10.

He, J., Cui, A., Ni, F., Deng, S., Shen, F. and Yang, G. (2018) 'A novel 3D yttrium based-graphene oxide-sodium alginate hydrogel for remarkable adsorption of fluoride from water', *Journal of Colloid and Interface Science*, Vol. 531, pp.37–46.

Hernandez, M., Polo, A.M.S., Sanchez-Polo, M., Rivera-Utrilla., Berber-Mendoza, M.S., Andrade-Espinosa, G. and Lopez-Ramon, M.V. (2019) 'Lanthanum-doped silica xerogels for the removal of fluorides from waters', *J. Environ. Manag.*, Vol. 213, pp.549–554.

Imran, A., Gupta, V.K., Khan, T.A. and Asim, M. (2012) 'Removal of arsenate from aqueous solution by electro-coagulation method using Al-Fe electrodes', *International Journal of Electrochemical Science*, Vol. 7, No. 3, pp.1898–1907.

Ingallinella, A.M., Virginia, A.P., Rub, E., Fernandez, G. and Vidoni, R.M. (2011) 'Graciela sanguinetti, simultaneous removal of arsenic and fluoride from groundwater by coagulation-adsorption with polyaluminum chloride', *Journal of Environmental Science and Health*, Vol. 46, No. 11, pp.1288–1296.

Jayarathna, L., Bandara, A., Ng, W.J. and Weerasooriya, R. (2015) 'Fluoride adsorption on γ-Fe_2O_3 nanoparticles', *Journal of Environmental Health Science and Engineering*, Vol. 13, No. 54, pp.1–10.

Jethave, G., Fegade, U., Rathod, R. and Pawar, J. (2018) 'Dye pollutants removal from wastewater using metal oxide nanoparticle embedded activated carbon: an immobilization study', *Journal of Dispersion Science and Technology*, Vol. 40, No. 4, pp.563–573.

Kacho, H.A., Nia, H.A. and Farhad, P. (2020) *Removal of Color from Hospital Wastewater with Activated Nanobiocarbon Derived from the Pit of the Olea woodiana (Forest Olive): Kinetics and Isotherms Study*, Vol. 26, No. 2, pp.245–258.

Khani, H., Rofouei, M.K., Arab, P., Gupta, V.K. and Vafaei, Z. (2010) 'Multi-walled carbon nanotubes-ionic liquid-carbon paste electrode as a super selectivity sensor: application to potentiometric monitoring of mercury ion(II), *Journal of Hazardous Materials*, Vol. 183, Nos. 1–3, pp.402–409.

Khorshidi, N. and Azadmehr, A.R. (2016) 'Characterisation and adsorption properties of oxalate-loaded hematite composite for Cd(II) and Pb(II) adsorption: equilibrium models thermodynamic and kinetic studies', *Separation Science and Technology*, Vol. 51, No. 13, pp.2122–2137.

Kimambo, V., Bhattacharya, P., Mtalo, F., Mtamba, J. and Ahmad, A. (2019) 'Fluoride occurrence in groundwater systems at global scale and status of defluoridation – state of the art', *Groundwater for Sustainable Development*, Vol. 9, p.100223.

Konale, R., Mahale, N. and Ingle, S. (2020) 'Nano-zeolite-graphene oxide composite for calcium hardness removal: isotherm and Kinetic study', *Water Practice and Technology*, Vol. 15, No. 4, pp.1011–1031.

Kuang, L., Liu, Y., Fu, D. and Zhao, Y. (2017) 'FeOOH-graphene oxide nanocomposites for fluoride removal from water: acetate mediated nano FeOOH growth and adsorption mechanism', *Journal of Colloid and Interface Science*, Vol. 490, pp.259–269.

Li, Y., Du, Q., Wang, J., Liu, T., Sun, J., Wang, Y., Wang, Z., Xia, Y. and Xia, L. (2013) 'Defluoridation from aqueous solution by manganese oxide coated graphene oxide', *Journal of Fluorine Chemistry*, Vol. 148, pp.67–73.

Li, Y., Zhang, P., Du, Q., Peng, X., Liu, T., Wang, Z., Xia, Y., Zhang, W., Wang, K., Zhu, H. and Wu, D. (2011) 'Adsorption of fluoride from aqueous solution by graphene', *Journal of Colloid and Interface Science*, Vol. 363, No. 1, pp.348–354.

Liu, L., Cui, Z., Ma, Q., Cui, W. and Zhang, Z. (2016a) 'One-step synthesis of magnetic iron-aluminum oxide/graphene oxide nanoparticles as a selective adsorbent for fluoride removal from aqueous solution', *RSC Advances*, Vol. 6, No. 13, pp.10783–10791.

Liu, Y., Lv, J., Jin, W. and Zhao, Y. (2016b) 'Defluoridation by rice spike-like akaganeite anchored graphene oxide', *RSC Advances*, Vol. 6, No. 14, pp.11240–11249.

Mahale, N.K. and Ingle, S.T. (2017) 'Electrocatalytic hydrogen evolution reaction on nano-nickel decorated graphene electrode', *Energy*, Vol. 119, No. C, pp.872–878.

Malana, M.A., Muhammad, J.D., Ashiq, M.N. and Gohar, R.S. (2014) 'Defluoridation of aqueous solutions by nanocomposite of MgAl2O4 and MA-VA-AA polymer: kinetics and mechanism', *Desalination and Water Treatment*, Vol. 55, No. 6, pp.1629–1638.

Manikandan, S., Chidambaram, S., Ramanathan, A.L., Prasanna, M.V., Thivya, C., Karmegam, U., Thiagavathi, R. and Rajkumar, K. (2013) 'A study on the defluoridation in water by using natural soil', *Applied Water Science*, Vol. 3, pp.741–751.

Manna, S., Gopakumar, D.A., Roy, D., Saha, P. and Thomas, S. (2018) 'Nanobiomaterials for removal of fluoride and chlorophenols from water', *New Polymer Nanocomposites for Environmental Remediation*, pp.487–498.

Marcano, D.C., Kosynkin, D.V., Berlin, J.M., Zhengzong, A.S., Slesarev, A., Alemany, L.B., Lu, W. and Tour, J.M. (2010) 'Improved synthesis of graphene oxide', *ACS Nano*, Vol. 4, No. 8, pp.4806–4814.

Marin, P., Modenes, A.N., Bergamasco, R., Paraiso, P.R. and Hamoudi, S. (2016) 'Synthesis, characterization and application of zrcl4-graphene composite supported on activated carbon for efficient removal of fluoride to obtain drinking water', *Water Air Soil Pollution*, Vol. 227, No. 12, pp.1–15.

Martinez, L., Kharissova, O.V. and Kharisov, B. (2019) *Handbook of Ecomaterials*, Springer International Publishing, Switzerland.

Melidis, P. (2015) 'Fluoride removal from aluminium finishing wastewater by hydroxyapatite', *Environ Process*, Vol. 2, pp.205–213.

Mesquita, G.L., Tanaka, F.O., Cantarella, H. and Mattos, D. (2011) 'Atmospheric absorption of fluoride by cultivated species leaf structural changes and plant growth', *Water, Air, and Soil Pollution*, Vol. 219, No. 1, pp.143–156.

Minju, K., Swaroop, V., Haribabu, K., Sivasubramanian, V. and Senthil Kumar, P. (2013) 'Removal of fluoride from aqueous media by magnesium oxide-coated nanoparticles', *Desalination and Water Treatment*, Vol. 53, No. 11, pp.2905–2914.

Mittal, A., Mittal, J., Malviya, A. and Gupta, V.K. (2010) 'Removal and recovery of Chrysoidine Y from aqueous solutions by waste materials', *Journal of Colloid and Interface Science*, Vol. 344, No. 2, pp.497–507.

Mohammadi, N., Khani, H., Gupta, V.K., Amereh, E. and Agarwal, S. (2011) 'Adsorption process of methyl orange dye onto mesoporous carbon material–kinetic and thermodynamic studies', *Journal of Colloid and Interface Science*, Vol. 362, No. 2, pp.457–462.

Mudila, H., Zaidi, M.H., Rana, S. and Alam, S. (2016) 'Comparative electrochemical study of sulphonated polysulphone binded graphene oxide supercapacitor in two electrolytes', *CARBON Letters*, Vol. 18, pp.43–48.

Mudzielwana, R., Gitari, W.M., Akinyemi, S.A. and Msagati, T.A. (2017) 'Synthesis, characterization, and potential application of Mn2+– intercalated bentonite in fluoride removal: adsorption modeling and mechanism evaluation', *Applied Water Science*, Vol. 7, No. 8, pp.4549–4561.

Mukhopadhyay, K., Ghosh, U.C. and Sasikumar, P. (2019) 'Enhanced capacity of fluoride scavenging from contaminated water by nano-architectural reorientation of cerium-incorporated hydrous iron oxide with graphene oxide', *Environmental Science and Pollution Research*, Vol. 26, No. 25, pp.26112–26133.

Nabbou, N., Belhachemi, M., Boumelik, M., Merzougui, T., Lahcene, D., Harek, Y., Zorpas, A. and Jeguirim, M. (2018) 'Removal of fluoride from groundwater using natural clay (kaolinite): optimization of adsorption conditions', *Comptes Rendus–Chimie*, Vol. 22, Nos. 2–3, pp.105–112.

Nekouei, F., Nekouei, S., Tayagi, I. and Gupta, V.K. (2015) 'Kinetic, thermodynamic and isotherm studies for acid blue 129 removal from liquids using copper oxide nanoparticle modified activated carbon as a novel adsorbent', *Journal of Molecular Liquids*, Vol. 201, pp.124–133.

Nigri, E.M., Cechinel, M.P., Mayer, D.A., Mazur, L.P., Loureiro, J.M., Rocha, S.F. and Vilar, V.P. (2017) 'Cow bones char as a green sorbent for fluorides removal from aqueous solutions: batch and fixed-bed studies', *Environmental Science and Pollution Research*, Vol. 24, pp.2364–2380.

Pandi, K. and Viswanathan, N. (2016) 'A facile synthesis of metal ion-imprinted graphene oxide/alginate hybrid 1 biopolymeric beads for enhanced fluoride sorption', *RSC Adv.*, Vol. 6, No. 79, pp.75905–75915.

Pourbeyram, S. (2019) 'Effective removal of heavy metals from aqueous solutions by graphene oxide-zirconium phosphate (GO-Zr-P) nanocomposite', *Industrial and Engineering Chemistry Research*, Vol. 55, No. 19, pp.5608–5617.

Prabhu, S.M., Elanchezhiyan, S.S., Lee, G. and Meenakshi, S. (2016) 'Defluoridation of water by graphene oxide supported needle-like complex adsorbents', *Journal of Inorganic and Organometallic Polymers and Materials*, Vol. 26, No. 4, pp.834–844.

Rajendran, S., Khan, M.M., Gracia, F., Qin, J., Gupta, V.K. and Arumainathan, S. (2016) 'Ce3+–ion-induced visible-light photocatalytic degradation and electrochemical activity of ZnO/CeO_2 nanocomposite', *Scientific Reports*, Vol. 6, p.31641.

Rao, P.N., Rao, A.D., Bhargav, J.S., Siva Sankar, K. and Sudharshan, G. (2014) 'Regional appraisal of the fluoride occurrence in ground-waters of Andhra Pradesh', *Journal of Geological Society of India*, Vol. 84, pp.483–493.

Saleh, T.A. and Gupta, V.K. (2011) 'Functionalization of tungsten oxide into MWCNT and its application for sunlight-induced degradation of rhodamine B', *Journal of Colloid and Interface Science*, Vol. 362, No. 2, pp.337–344.

Saleh, T.A. and Gupta, V.K. (2012) 'Photo-catalysed degradation of hazardous dye methyl orange by use of a composite catalyst consisting of multi-walled carbon nanotubes and titanium dioxide', *Journal of Colloid and Interface Science*, Vol. 371, No. 1, pp.101–106.

Saleh, T.A. and Gupta, V.K. (2012) 'Synthesis and characterization of alumina nano-particles polyamide membrane with enhanced flux rejection performance', *Separation and Purification Technology*, Vol. 89, pp.245–251.

Saleh, T.A. and Gupta, V.K. (2014) 'Processing methods, characteristics and adsorption behavior of tires derived carbons: a review', *Advances in Colloid and Interface Science*, Vol. 211, pp.92–101.

Saravanan, R., Gupta, V.K., Prakash, T., Narayanan, V. and Stephen, A. (2013) 'Synthesis, characterization and photocatalytic activity of novelHg doped ZnO nanorods prepared by thermal decomposition method', *Journal of Molecular Liquids*, Vol. 178, pp.88–93.

Saravanan, R., Joicy, S., Gupta, V.K., Narayanan, V. and Stephen, A. (2013) 'Visible light induced degradation of methylene blue using CeO_2/V_2O_5 and CeO_2/CuO catalysts', *Materials Science and Engineering C*, Vol. 33, No. 8, pp.4725–4731.

Saravanan, R., Karthikeyan, N., Gupta, V.K., Thirumal, E., Thangadurai, P., Narayanan, V. and Stephen, A. (2013) 'ZnO/Ag nanocomposite: an efficient catalyst for degradation studies of textile effluents under visible light', *Materials Science and Engineering C*, Vol. 33, No. 4, pp.2235–2244.

Saravanan, R., Karthikeyan, S., Gupta, V.K., Sekaran, G., Narayanan, V. and Stephen, A. (2013) 'Enhanced photocatalytic activity of ZnO/CuO nanocomposite for the degradation of textile dye on visible light illumination', *Material Science and Engineering C*, Vol. 33, No. 1, pp.91–98.

Saravanan, R., Khan, M.M., Gupta, V.K., Mosquera, E., Gracia, F., Narayanan, V. and Stephen, A. (2012) '$ZnO/Ag/Mn_2O_3$ nanocomposite for visible light-induced industrial textile effluent degradation, uric acid and ascorbic acid sensing and antimicrobial activities', *RSC Advances*, Vol. 5, No. 44, pp.34645–34651.

Saravanan, R., Khan, M.M., Gupta, V.K., Mosquera, V., Gracia, F., Narayanan, V. and Stephen, A. (2015) 'ZnO/Ag/CdO nanocomposite for visible light-induced photocatalytic degradation of industrial textile effluents', *Journal of Colloid and Interface Science*, Vol. 452, pp.126–133.

Saravanan, R., Sacari, E., Gracia, F., Khan, M.M., Mosquera, E. and Gupta, V.K. (2016) 'Conducting PANI stimulated ZnO system for visible light photocatalytic degradation of coloured dyes', *Journal of Molecular Liquids*, Vol. 221, pp.1029–1033.

Saravanan, R., Thirumal, E., Gupta, V.K., Narayanan, V. and Stephen, A. (2013) 'The photocatalytic activity of ZnO prepared by simple thermal decomposition method at various temperatures', *Journal of Molecular Liquids*, Vol. 177, pp.394–401.

Selvan, K.H. and Sundari, P.M. (2020) 'An equilibrium and kinetic study for the removal of reactive red M5B using phosphoric acid treated activated carbon', *International Journal of Environment and Waste Management*, Vol. 26, No. 1, pp.39–58.

Shang, Y., Wang, Z., Xu, X., Gao, B., Yue, Q., Liu, S. and Han, C. (2019) 'Enhanced fluoride uptake by bimetallic hydroxides anchored in cotton cellulose/graphene oxide composites', *Journal of Hazardous Materials*, Vol. 376, pp.91–101.

Singh, G., Sinam, G., Kriti, Pandey, M., Kumari, B. and Kulsoom, M. (2020) 'Soil pollution by fluoride in india: distribution, chemistry and analytical methods', in Shukla, V. and Kumar, N. (Eds.): *Environmental Concerns and Sustainable Development*, Springer, Singapore [online] https://doi.org/10.1007/978-981-13-6358-0_12.

Singh, K., Lataye, D.H. and Wasewar, K.L. (2017) 'Removal of fluoride from aqueous solution by using Bael (Aegle marmelos) shell activated carbon: kinetic, equilibrium and thermodynamic study', *Journal of Fluorine Chemistry*, Vol. 194, pp.23–32.

Suhas, Gupta, V.K., Carrott, P.J.M., Singh, R., Chaudhary, M. and Kushwaha, S. (2016) 'Cellulose: a review as natural, modified, and activated carbon adsorbent', *Bioresource Technology*, Vol. 216, pp.1066–1076.

Tabish, T.A., Memon, F.A., Gomez, D.E., Horsell, D.W. and Zhang, S. (2018) 'A facile synthesis of porous graphene for efficient water and wastewater treatment', *Scientific Reports*, Vol. 8, p.1817.

Tirkey, P., Bhattacharya, T. and Chakraborty, S. (2017) 'Optimization of fluoride removal from aqueous solution using Jamun (Syzygium cumini) leaf ash', *Process Safety and Environment Protection*, Vol. 115, pp.125–138.

Tomar, V. and Kumar, D. (2013) 'A critical study on efficiency of different materials for fluoride removal from aqueous media', *Journal of Chemistry Central*, Vol. 7, No. 57, p.51.

Vardhan, V.M. and Srimurali, M. (2016) 'Removal of fluoride from water using a novel sorbent lanthanum-impregnated bauxite', *Springer Plus*, Vol. 5, p.1426.

WHO Guidelines for Drinking Water-Quality (2004) *IPCS 2002, Environmental Health Criteria 227 Fluorides*, World Health Organization, Geneva.

Wu, K., Chen, Y., Ouyang, Y., Lei, H. and Liu, T. (2018) 'Adsorptive removal of fluoride from water by granular zirconium-aluminum hybrid adsorbent: performance and mechanisms', *Environmental Science and Pollution Research*, Vol. 25, No. 16, pp.15390–15403.

Xie, Z., Yang, B., Yang, L., Xu, X., Cai, D., Chen, J., Chen, Y., He, Y., Li, Y. and Zhou, X. (2015) 'Addition of graphene oxide into graphite toward effective positive electrode for advanced zinc-cerium redox flow battery', *Journal of Solid State Electrochem.*, Vol. 19, No. 11, pp.3339–3345.

Xu, C., Li, J., He, F., Cui, Y., Huang, C., Jin, H. and Hou, S. (2016) 'Al_2O_3-Fe_3O_4-expanded graphite nano-sandwich structure for fluoride removal from aqueous solution', *RSC Advances*, Vol. 6, No. 99, pp.97376–97384.

Xu, N., Li, S., Li, W. and Liu, Z. (2020) 'Removal of fluoride by graphene oxide/alumina nanocomposite: adsorbent preparation, characterization, adsorption performance and mechanisms', *Chemistry Select*, Vol. 5, No. 6, pp.1818–1828.

Yin, H., Kong, M. and Tang, W. (2015) 'Removal of fluoride from contaminated water using natural calcium-rich attapulgite as a low-cost adsorbent', *Water, Air, and Soil Pollution*, Vol. 226, pp.1–11.

Yu, H., Zhang, B., Bulin, C., Li, R. and Xing, R. (2016) 'High-efficient synthesis of graphene oxide based on improved hummers method', *Scientific Reports,* Vol. 6, p.36143.

Zhang, R., Cai, Y., Zhu, X., Han, Q., Zhang, T., Liu, Y., Li, Y. and Wang, A. (2018) 'A novel photocatalytic membrane decorated with PDA/RGO/Ag_3PO_4 for catalytic dye decomposition', *Colloids and Surfaces A: Physicochem. Eng. Aspects*, Vol. 563, pp.68–76.

Zhou, J., Yu, J., Liao, H., Zhang, Y. and Luo, X. (2019) Facile fabrication of bimetallic collagen fiber particles via immobilizing zirconium on chrometanned leather as adsorbent for fluoride removal from ground water near hot spring', *Separation Science and Technology*, Vol. 55, No. 4, pp.658–671.

Zhou, X., Bai, Z., Wu, M., Qiao, J. and Chen, Z. (2015) '3-dimensional porous n-doped graphene foam as a non-precious catalyst for the oxygen reduction reaction', *Journal of Materials Chemistry A*, Vol. 3, No. 7, pp.3343–3353.